Impulse approximation *NN* amplitudes for proton-nucleus interactions

J. A. McNeil
Department of Physics, Villanova University, Villanova, Pennsylvania 19085
and Department of Physics, University of Pennsylvania, Philadelphia, Pennsylvania 19104

L. Ray
Department of Physics, University of Texas, Austin, Texas 78712

S. J. Wallace
Department of Physics and Astronomy, University of Maryland, College Park, Maryland 20742
(Received 10 January 1983)

Transformations of nucleon-nucleon amplitudes from the center of mass frame to the proton-nucleus Breit frame are developed for use in multiple scattering analyses. As a by product, a matrix equation is given for the invariant *NN* amplitudes in Dirac spinor representation. Based on recent *NN* phase shifts, Gaussian parametrization of the *pp* and *np* amplitudes are calculated and some proton-nucleus calculations are presented to illustrate the effects of the Breit frame amplitudes. For ^{40}Ca, these effects are quite small.

NUCLEAR REACTIONS Nucleon-nucleon amplitudes, impulse approximation, Breit frame, Wigner rotation, Dirac invariant amplitudes, proton-nucleus elastic scattering.

Intermediate energy proton-nucleus elastic scattering is qualitatively explained by the impulse approximation, as has been shown in many analyses.[1,2] In multiple scattering theory, the impulse approximation consists of the use of free nucleon-nucleon (*NN*) scattering amplitudes without corrections for off-shell effects or for the influence of the nuclear medium. Gurvitz, Dedonder, and Amado[3,4] have defined an optimal impulse approximation in which leading order corrections due to Fermi motion are shown to vanish provided that the *NN* amplitude commutes with the nuclear potential. This is expected to be a good approximation because the *NN* amplitudes which determine the single scattering optical potential do not involve the spin of nucleons in the nucleus and these amplitudes seem to be reasonably local (i.e., they depend mainly on momentum transfer, $\vec{q}$).

Working in the proton-nucleus center of mass (c.m.) system, the single scattering approximation to the proton-nucleus elastic scattering amplitude corresponds to the diagram of Fig. 1:

$$F^{(1)}(\vec{k},\vec{k}';T_L)=-\frac{k}{2\pi v_L}\sum_j (2\pi)^{-3}\int d^3p\,\psi_j^*\left[\vec{p}+\tfrac{1}{2}\vec{q}-\frac{1}{A}\vec{k}_a\right]$$
$$\times\left\langle \vec{k}_a-\tfrac{1}{2}\vec{q};\vec{p}+\tfrac{1}{2}\vec{q}-\frac{1}{A}\vec{k}_a\,\middle|\,t(T_L-H)\,\middle|\,\vec{k}_a+\tfrac{1}{2}\vec{q};\vec{p}-\tfrac{1}{2}\vec{q}-\frac{1}{A}\vec{k}_a\right\rangle$$
$$\times\psi_j\left[\vec{p}-\tfrac{1}{2}\vec{q}-\frac{1}{A}\vec{k}_a\right], \qquad (1)$$

where $\vec{k}_a\equiv\frac{1}{2}(\vec{k}+\vec{k}')$ and $\vec{q}\equiv\vec{k}-\vec{k}'$ are the average of initial and final proton momenta and the momentum transfer, respectively. T_L is the laboratory proton energy, H represents the nuclear Hamiltonian, and v_L is the laboratory velocity of the proton. The single-particle wave functions ψ_j depend on the struck nucleon momentum relative to the nuclear center of mass. In principle, off-shell *NN* t-matrix elements are needed to evaluate Eq. (1). However, as already noted, the important t-matrix elements seem reasonably local. Furthermore, the variation of the *NN* t matrix with momentum $\vec{p}$ in the integral of Eq. (1) is compensated to leading order in $\vec{p}/m$ by appropriate choice of the energy parameter upon which the t matrix depends. This is the optimal impulse approximation of Refs. 3 and 4. The condition on the energy is that the *NN* t matrix be on shell when evaluated at $\vec{p}=0$ in Fig. 1 or Eq. (1). We refer to the $\vec{p}=0$ situation as the Breit frame [see Fig. 2(a)].

Approximating the t matrix by its value at $\vec{p}=0$ in Eq. (1) permits it to be taken outside the integral and the remaining integration produces the nuclear form factor (normalized to the number of nucleons)

$$S(\vec{q})=\sum_j (2\pi)^{-3}\int d^3p\, \psi_j^*\left[\vec{p}+\tfrac{1}{2}\vec{q}-\frac{1}{A}\vec{k}_a\right]\psi_j\left[\vec{p}-\tfrac{1}{2}\vec{q}-\frac{1}{A}\vec{k}_a\right] . \tag{2}$$

Thus the optimal approximation produces the following factorized form for elastic scattering by a spin saturated nucleus:

$$F^{(1)}(\vec{k},\vec{k}',E)=\tfrac{1}{2}\mathrm{Tr}_{\sigma_2} f_B(\vec{k},\vec{k}')S(\vec{q}) , \tag{3}$$

where the Breit frame NN amplitude, f_B, is related to the t matrix by

$$f_B(\vec{k},\vec{k}')=-\frac{k}{2\pi v_L}\left\langle \vec{k}_a-\tfrac{1}{2}\vec{q};\tfrac{1}{2}\vec{q}-\frac{1}{A}\vec{k}_a \,\middle|\, t(T_L^{\mathrm{eff}}) \,\middle|\, \vec{k}_a+\tfrac{1}{2}\vec{q};-\tfrac{1}{2}\vec{q}-\frac{1}{A}\vec{k}_a\right\rangle , \tag{4}$$

and T_L^{eff} denotes the energy parameter appropriate to the Breit frame [Eq. (6) below]. The trace over spins of the struck nucleon [labeled 2 in Eq. (3)] eliminates all but scalar and single spin-flip terms in f_B; however, for inelastic scattering, other spin components of f_B may contribute. When transformed to coordinate space, Eq. (3) is seen to be equivalent to the "$t\rho$" approximation commonly used for the first-order optical potential with the optimality condition being that the Breit frame NN amplitude is to be used. A complete treatment of the optical potential can be made based on the diagram of Fig. 1 except that in general the nucleons are not on mass shell. Usually this complication is avoided by using a first-order optical potential equal to Eq. (3) except for kinematical factors. This line of reasoning leads to the conclusion that the impulse approximation optical potential should be based on the Breit frame amplitude.

Since the Breit frame amplitude is on shell, it can be related to the c.m. amplitude at the same invariant energy and momentum transfer. From Fig. 2(a), the square of the total four-momentum of the two nucleons is calculated to be

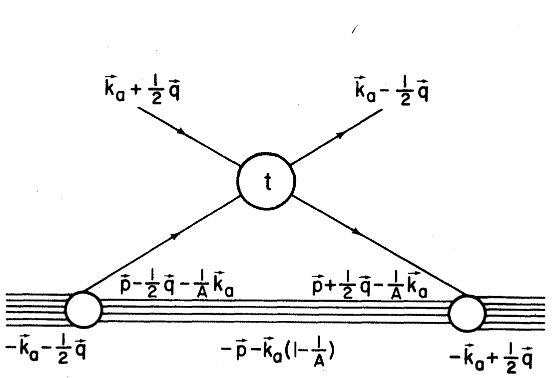

FIG. 1. Impulse approximation for elastic proton-nucleus scattering. $\vec{k}$ is the proton-nucleus center-of-mass momentum.

$$s_B(q^2)=\left[E(\vec{k})+E\left[-\tfrac{1}{2}\vec{q}-\frac{1}{A}\vec{k}_a\right]\right]^2 - \left[\vec{k}_a\left[1-\frac{1}{A}\right]\right]^2 , \tag{5}$$

where

$$E(\vec{k})=(k^2+m^2)^{1/2} .$$

For fixed momentum $\vec{k}$ in the proton-nucleus c.m. the q^2 dependence in $s_B(q^2)$ causes the Breit frame amplitude to be evaluated at an effective laboratory energy given by[5]

$$T_L^{\mathrm{eff}}\equiv\frac{s_B(q^2)-4m^2}{2m} . \tag{6}$$

The situation corresponds to the beam proton striking a nucleon with "optimal" Fermi momentum $-\frac{1}{2}\vec{q}-(1/A)\vec{k}_a$ which invariably increases the energy, i.e.,

$$T_L^{\mathrm{eff}}(q^2)>T_L(0)\equiv T_L ,$$

where T_L is the incident proton kinetic energy in the laboratory frame. The two-body scattering is then calculated under the assumption that the struck nucleon is on mass shell.

In the following, we present two procedures for calculating the Breit frame NN amplitudes. The first procedure is more cumbersome but has the important by-product of providing a means of calculating Dirac invariant NN amplitudes directly from the NN phase shifts. A very brief outline of the method has been given in Ref. 2 and a more detailed treatment can be found in Ref. 6. The second method involves a Wigner rotation and is essentially the same as discussed in Ref. 7. For completeness a derivation of the Wigner transformation is outlined.

Assuming isospin conservation, the strong interaction scattering matrix can be expressed in terms of five complex amplitudes for pp and five more for *np*. A convenient parametrization in the *NN* center-of-mass frame is

$$(2ik_c)^{-1}f_c = A + B\vec{\sigma}_1\cdot\vec{\sigma}_2 + iqC(\sigma_{1n}+\sigma_{2n}) + D\vec{\sigma}_1\cdot\vec{q}\,\vec{\sigma}_2\cdot\vec{q} + E\vec{\sigma}_{1z}\sigma_{2z}\ , \qquad (7)$$

where $\hat{z}$ is a unit vector parallel to average momentum $\vec{k}_{ca}=\frac{1}{2}(\vec{k}_c+\vec{k}_c')$ and $\hat{n}=\hat{q}\times\hat{z}$. Subscripts 1 and 2 refer to the incident and struck nucleons, respectively. Amplitudes A, B, C, D, and E are regarded as known since they can be calculated from the *NN* phase shifts in a standard manner,[8] although it is necessary to account for the effective energy of Eq. (6).

For the purpose of transforming the *NN* amplitude from one frame to another, it is useful to introduce an invariant representation involving Dirac matrices γ^μ in place of the Pauli matrices $\vec{\sigma}$. One such representation is

$$\hat{\mathscr{F}} = \mathscr{F}_S + \mathscr{F}_V\gamma_1\cdot\gamma_2 + \mathscr{F}_T\sigma_2^{\mu\nu}\sigma_{2\mu\nu} + \mathscr{F}_P\gamma_1^5\gamma_2^5 + \mathscr{F}_A\gamma_1^5\gamma_1^\mu\gamma_2^5\gamma_{2\mu}\ , \qquad (8)$$

where the scalar ($\mathscr{F}_S$), vector ($\mathscr{F}_V$), tensor ($\mathscr{F}_T$), pseudoscalar ($\mathscr{F}_P$), and axial vector ($\mathscr{F}_A$) Dirac amplitudes are functions of the Lorentz invariants s and $t\equiv -q^2$. An alternative representation is discussed in Ref. 9. Matrix elements of $\hat{\mathscr{F}}$ between initial and final Dirac spinors appropriate to Fig. 2(b) are equivalent to matrix elements of f_c between corresponding initial and final Pauli spinors, χ_s, as follows:

$$\bar{u}_{s_1'}(\vec{k}_c')\bar{u}_{s_2'}(-\vec{k}_c')\hat{\mathscr{F}}u_{s_1}(\vec{k}_c)u_{s_2}(-\vec{k}_c) = \chi_{s_1'}^{+}\chi_{s_2'}^{+}[(2ik_c)^{-1}f_c]\chi_{s_1}\chi_{s_2}\ , \qquad (9)$$

where

$$u_s(\vec{k}) = L(\vec{k})\begin{bmatrix}\chi_s\\ 0\end{bmatrix} \qquad (10)$$

and

$$L(\vec{k}) = \left[\frac{E(\vec{k})+m}{2m}\right]^{1/2}\begin{bmatrix}1 & \dfrac{\vec{\sigma}\cdot\vec{k}}{E(\vec{k})+m}\\ \dfrac{\vec{\sigma}\cdot\vec{k}}{E(\vec{k})+m} & 1\end{bmatrix}. \qquad (11)$$

$L(\vec{k})$ is a Lorentz boost operator for Dirac spinors.[10] Equations (7)–(9) define a matrix relation between the Pauli and Dirac *NN* amplitudes:

$$\begin{bmatrix}A\\B\\C\\D\\E\end{bmatrix}_{\text{c.m.}} = 0(\vec{k}_c;1)\begin{bmatrix}\mathscr{F}_S\\ \mathscr{F}_V\\ \mathscr{F}_T\\ \mathscr{F}_P\\ \mathscr{F}_A\end{bmatrix}\ , \qquad (12)$$

where $0(\vec{k}_c;1)$ is a 5×5 matrix to be specified shortly. Given the Pauli amplitudes, this matrix may be inverted to determine the Dirac amplitudes.

From the Dirac amplitudes, one can determine the Breit frame amplitude corresponding to Fig. 2(a) by a relation similar to Eq. (9):

$$\bar{u}_{s_1'}(\vec{k}')\bar{u}_{s_2'}\left[\tfrac{1}{2}\vec{q}-\frac{1}{A}\vec{k}_a\right]\hat{\mathscr{F}}u_{s_1}(\vec{k})u_{s_2}\left[-\tfrac{1}{2}\vec{q}-\frac{1}{A}\vec{k}_a\right] = \chi_{s_1'}^{+}\chi_{s_2'}^{+}[(2ik_B)^{-1}f_B]\chi_{s_1}\chi_{s_2}\ . \qquad (13)$$

This relation fixes the form of the Breit frame amplitude to be

$$(2ik_B)^{-1}f_B = A + B\vec{\sigma}_1\cdot\vec{\sigma}_2 + iq(C_1\sigma_{1n}+C_2\sigma_{2n}) + D\vec{\sigma}_1\cdot\vec{q}\,\vec{\sigma}_2\cdot\vec{q} + E\sigma_{1z}\sigma_{2z}\ . \qquad (14)$$

Note that six complex amplitudes are present in the Breit frame whereas only five are needed in the c.m. frame. Owing to time reversal invariance, the coefficients of σ_{1n} and σ_{2n} are identical in Eq. (7). There are two different coefficients in Eq. (14) because the momenta of Fig. 2(a) do not transform into one another under time reversal. As before, Eqs. (13) and (14) imply a matrix relation,

$$\begin{bmatrix}A\\B\\C_1\\C_2\\D\\E\end{bmatrix}_{\text{Breit}} = 0(\vec{k};A)\begin{bmatrix}\mathscr{F}_S\\ \mathscr{F}_V\\ \mathscr{F}_T\\ \mathscr{F}_P\\ \mathscr{F}_A\end{bmatrix}\ , \qquad (15)$$

where $0(\vec{k};A)$ is a 6×5 matrix for $A>1$.

Solving Eq. (12) for the Dirac amplitudes leads to a direct relation between the (known) c.m. and the unknown Breit amplitudes:

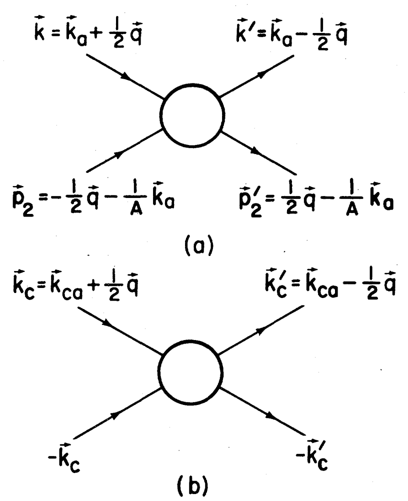

FIG. 2. (a) Breit frame *NN* scattering. (b) *NN* c.m. frame scattering.

$$\begin{bmatrix} A \\ B \\ C_1 \\ C_2 \\ D \\ E \end{bmatrix}_{\text{Breit}} = 0(\vec{k};A)0^{-1}(\vec{k}_c;1)\begin{bmatrix} A \\ B \\ C \\ D \\ E \end{bmatrix}_{\text{c.m.}} . \qquad (16)$$

The general 6×5 matrix $0(\vec{k};A)$ is defined in Tables I and II. From this matrix, the 5×5 matrix, $0(\vec{k}_c;1)$, is obtained by (i) replacing $\vec{k}$ by the c.m. momentum $\vec{k}_c$, (ii) setting $A=1$, and (iii) deleting the fourth row. In the limit $A=1$ and $\vec{k}=\vec{k}_c$, the two amplitudes C_1 and C_2 of Eq. (14) become identical and one of them may be simply eliminated to obtain the matrix $0(\vec{k}_c;1)$.

In the case where the invariant energy for *NN* scattering is the same in the c.m. and Breit frames, the c.m. momentum is determined by

$$k_c=[\tfrac{1}{4}s_B(q^2)-m^2]^{1/2} , \qquad (17)$$

which also corresponds to using the effective laboratory energy of Eq. (6). The relation between c.m. and Breit frame amplitudes is a Wigner rotation of the spins. The Wigner rotation may be expressed as a 6×5 matrix equivalent to

$$W=0(\vec{k};A)0^{-1}(\vec{k}_c;1)\,|_{s_B=s_c} . \qquad (18)$$

The notation carries the reminder that the s value must be the same in the Breit and c.m. frames. Table III expresses the Wigner rotation matrix W in terms of two angles defined by

$$\tan(\tfrac{1}{2}\chi)=\frac{\tfrac{1}{2}qk_a\left[1-\dfrac{1}{A}\right]}{\sqrt{s_B}[\tfrac{1}{2}\sqrt{s_B}+E(\vec{p})+E(\vec{k})+m]} , \qquad (19)$$

TABLE I. The matrix $0(\vec{k};A)$ used in Eq. (15) of text. Formulas for matrix elements are given in Table II. To obtain the matrix $0(k_c;1)$ used in Eq. (12), row 4 of the table, corresponding to amplitude C_2, is omitted, the c.m. frame momentum $\vec{k}_c$ is used in place of $\vec{k}$ in Table II matrix elements, and the parameter A is unity. The momentum transfer q is the same in both cases.

A	=	x_1x_2	$x_3x_4+x_5$	$-2x_6(1+x_7)$	0	x_6x_7	$\mathscr{F}_S$
B		$-x_6x_7$	$-x_6(1+x_7)$	$2x_5+2x_3x_4$	0	$-x_1x_2$	$\mathscr{F}_V$
C_1		x_2x_8	$-x_4x_8-\dfrac{k_a}{2Am^2}$	$-2x_3x_9-\dfrac{k_a}{m^2}$	0	$-x_1x_9$	$\mathscr{F}_T$
C_2		x_1x_9	$-x_3x_9-\dfrac{k_a}{2m^2}$	$-2x_4x_8-\dfrac{k_a}{Am^2}$	0	$-x_2x_8$	
D		$\dfrac{x_7}{4m^2}$	$\dfrac{1+x_7}{4m^2}$	x_{10}	$-\dfrac{1}{4m^2}$	x_{11}	$\mathscr{F}_P$
E		x_6x_7	x_6x_7	x_{12}	0	x_{13}	$\mathscr{F}_A$

TABLE II. Matrix element formulas for given values of q, the momentum transfer, and $k_a=1/2(\vec{k}+\vec{k}')$. Note that $\vec{k}_a\cdot\vec{q}=0$ holds for elastic proton-nucleus scattering and for elastic *NN* scattering.

$E_1=[m^2+k_a^2+(\frac{1}{4})q^2]^{1/2}$	$E_2=[m^2+(k_a^2/A^2)+(\frac{1}{4})q^2]^{1/2}$
$x_1=\frac{E_1+m}{2m}\left[1-\frac{k_a^2-(\frac{1}{4})q^2}{(E_1+m)^2}\right]$	$x_2=\frac{E_2+m}{2m}\left[1-\frac{(k_a^2/A^2)-(\frac{1}{4})q^2}{(E_2+m)^2}\right]$
$x_3=\frac{E_1+m}{2m}\left[1+\frac{k_a^2-(\frac{1}{4})q^2}{(E_1+m)^2}\right]$	$x_4=\frac{E_2+m}{2m}\left[1+\frac{(k_a^2/A^2)-(\frac{1}{4})q^2}{(E_2+m)^2}\right]$
$x_5=\frac{k_a^2}{Am^2}$	$x_6=\frac{q^2}{4m^2}$
$x_7=\frac{k_a^2}{A(E_1+m)(E_2+m)}$	$x_8=\frac{k_a}{2m(E_1+m)}$
$x_9=\frac{k_a}{2Am(E_2+m)}$	$x_{10}=\frac{x_3}{2m(E_2+m)}+\frac{x_4}{2m(E_1+m)}+\frac{x_6}{2(E_1+m)(E_2+m)}$
$x_{11}=\frac{x_1}{4m(E_2+m)}+\frac{x_2}{4m(E_1+m)}-\frac{x_6}{4(E_1+m)(E_2+m)}$	
$x_{12}=-2x_5(1-x_7)-\frac{2k_a^2x_3}{A^2m(E_2+m)}-\frac{2k_a^2x_4}{m(E_1+m)}$	
$x_{13}=-x_5(1+x_7)-\frac{k_a^2x_1}{A^2m(E_2+m)}-\frac{k_a^2x_2}{m(E_1+m)}$	

$$\tan(\tfrac{1}{2}\rho)=\frac{\frac{1}{2}qk_a\left[1-\frac{1}{A}\right]}{\sqrt{s_B}\left[\frac{1}{2}\sqrt{s_B}+E(\vec{p})+E\left[-\frac{1}{2}\vec{q}-\frac{1}{A}\vec{k}_a\right]+m\right]}\,, \tag{20}$$

where $k_a=|\vec{k}+\vec{k}'|/2$ and

$$E(\vec{p})=m\left[1+(k_a^2/s_B)\left[1-\frac{1}{A}\right]^2\right]^{1/2}.$$

The Wigner rotation limit provides the simplest connection between on-shell c.m. and Breit frame amplitudes. It also provides a nontrivial check on the 0 matrices since both sides of Eq. (18) can be independently calculated. The utility of the matrix 0 is mainly in providing the link between the (known) c.m. amplitudes and the invariant Dirac amplitudes of Eq. (8). A paper in preparation[11] shows that the phenomenological Dirac first-order optical potential is essentially the impulse approximation based on the Dirac amplitudes of Eq. (8).

The matrix W is derived by the following steps. Equations (9)—(11) can be solved for the Dirac amplitude $\hat{\mathscr{F}}$ by applying inverse boost operators [e.g., $\bar{u}(\vec{k})=\bar{u}(0)L(-\vec{k})$ since $\gamma^0L(k)\gamma^0=L(-\vec{k})=L^{-1}(\vec{k})$] as follows:

$$\hat{\mathscr{F}}=L_2(-\vec{k}_c')L_1(\vec{k}_c')\hat{M}_{\text{c.m.}}L_2(\vec{k}_c)L_1(-\vec{k}_c)\,, \tag{21}$$

where

$$\hat{M}_{\text{c.m.}}=(2ik_c)^{-1}\left[\frac{1+\gamma_1^0}{2}\right]f_c\left[\frac{1+\gamma_1^0}{2}\right]. \tag{22}$$

Since $\hat{\mathscr{F}}$ is Lorentz invariant, it is unaffected by further transformations. In particular, boost operators $L_1(\vec{p})$ and $L_2(\vec{p})$ which correspond to a boost from the c.m. frame of Fig. 2(b) into the Breit frame of Fig. 2(a) can be applied to $\hat{\mathscr{F}}$ yielding the invariance relation

$$\hat{\mathscr{F}}=L_1(\vec{p})L_2(\vec{p})\hat{\mathscr{F}}L_1(-\vec{p})L_2(-\vec{p})\,. \tag{23}$$

The boost momentum $\vec{p}$ connecting the c.m. and Breit frames is

$$\vec{p}=\left[\frac{m\vec{k}_a}{\sqrt{S_B}}\right]\left[1-\frac{1}{A}\right], \tag{24}$$

or equivalently, the boost velocity is $\vec{p}/E(\vec{p})$. The Breit frame amplitude defined by Eq. (13) is also related to the Dirac amplitude $\hat{\mathscr{F}}$ by boost operations as follows:

$$\hat{M}_B = L_1(-\vec{k}')L_2(-\vec{p}_2')\hat{\mathscr{F}}L_1(\vec{k})L_2(\vec{p}_2)\,, \quad (25)$$

where

$$\vec{p}_2 = -\tfrac{1}{2}\vec{q} - \frac{1}{A}\vec{k}_a$$

and

$$\vec{p}_2' = \tfrac{1}{2}\vec{q} - \frac{1}{A}\vec{k}_a\,,$$

and

$$\hat{M}_B = (2ik_B)^{-1}\left[\frac{1+\gamma_1^0}{2}\right]f_B\left[\frac{1+\gamma_2^0}{2}\right]. \quad (26)$$

Combining Eqs. (21), (23), and (25) yields

$$\hat{M}_B = L_1(-\vec{k}')L_2(-\vec{p}_2')L_1(\vec{p})L_2(\vec{p})L_2(-\vec{k}_c') \times L_1(\vec{k}_c')\hat{M}_{\text{c.m.}}L_2(\vec{k}_c)L_1(-\vec{k}_c)L_2(-\vec{p}) \times L_1(-\vec{p})L_2(\vec{p}_2)L_1(\vec{k})\,. \quad (27)$$

The boost operators $L(\vec{p})$ were inserted using Eq. (23) in order that the transformations would reduce to Wigner rotations of the spins, i.e., one can show that

$$L_1(-\vec{k}_c)L_1(-\vec{p})L_1(\vec{k}) = L_1(-\vec{k}')L_1(\vec{p})L_1(\vec{k}_c') = e^{i(1/2)\chi\sigma_{1n}}\,, \quad (28)$$

$$L_2(\vec{k}_c)L_2(-\vec{p})L_2(\vec{p}_2) = L_2(-\vec{p}_2')L_2(\vec{p})L_2(-\vec{k}_c') = e^{-i(1/2)\rho\sigma_{2n}}\,, \quad (29)$$

where χ and ρ are the angles defined by Eqs. (19) and (20). These results lead to the Wigner rotation form for the transformation of spin components of the NN amplitude

$$(2ik_B)^{-1}f_B = e^{i(1/2)\chi\sigma_{1n}}e^{-i(1/2)\rho\sigma_{2n}} \times (2ik_c)^{-1}f_c e^{i(1/2)\chi\sigma_{1n}}e^{-i(1/2)\rho\sigma_{2n}}\,. \quad (30)$$

Substituting the forms for f_c and f_B as given by Eqs. (7) and (14) leads, after some algebra, to the matrix W of Table III.

Calculations of the Breit frame NN amplitudes have been performed starting from a recent NN phase shift solution (SP82) of the Virginia Polytechnic Institute (VPI) group.[12] For elastic proton-nucleus scattering, Eq. (3), only the A and C_1 terms of Eq. (14) contribute due to the trace over spins. Nevertheless, all spin components of the Breit frame NN amplitudes have been tabulated in Table IV for pp and in Table V for np scattering. Generally the NN amplitudes enter into proton-nucleus analyses multiplied, as in Eq. (3), by a nuclear form factor $S(q)$. Since the form factor rapidly decreases with q, the most important range in which the NN amplitudes are needed is

$$0 < q^2 \lesssim (2\ \text{fm}^{-1})^2 = 0.16\ (\text{GeV}/c)^2\,.$$

In this range the amplitudes tend to be well approximated by Gaussian functions of q, e.g., $A(q) = A_0 e^{-\beta_A q^2}$, $C_1(q^2) = C_{10}e^{-\beta_{c_1}q^2}$, and so on, where $A(q)$ and $C_1(q)$ are defined as in Eq. (14). The tables give numerical values of these Gaussian parameters applicable to the range $0° < \theta_{\text{c.m.}} < 40°$. In the case of the double spin flip amplitude E, the q

TABLE III. Wigner rotation matrix. The angles χ and ρ are defined by Eqs. (19) and (20).

$$\begin{bmatrix} A \\ B \\ C_1 \\ C_2 \\ D \\ E \end{bmatrix}_{Br} = \begin{bmatrix} \cos\chi\cos\rho & \sin\chi\sin\rho & -q\sin(\chi-\rho) & 0 & 0 \\ \sin\chi\sin\rho & \cos\chi\cos\rho & -q\sin(\chi-\rho) & 0 & 0 \\ \frac{\sin\chi\cos\rho}{q} & -\frac{\cos\chi\sin\rho}{q} & \cos(\chi-\rho) & 0 & 0 \\ -\frac{\cos\chi\sin\rho}{q} & \frac{\sin\chi\cos\rho}{q} & \cos(\chi-\rho) & 0 & 0 \\ -\frac{\sin\chi\sin\rho}{q^2} & \frac{1-\cos\chi\cos\rho}{q^2} & \frac{\sin(\chi-\rho)}{q} & 1 & 0 \\ -\sin\chi\sin\rho & 1-\cos\chi\cos\rho & q\sin(\chi-\rho) & 0 & 1 \end{bmatrix} \begin{bmatrix} A \\ B \\ C \\ D \\ E \end{bmatrix}_{\text{c.m.}}$$

TABLE IV. *pp* Breit frame Gaussian amplitude parameters for the amplitudes of Eq. (14). Forward ($q=0$) amplitudes A_0, B_0, and E_0 are in units of $(\text{GeV}/c)^{-2}$, C_{10} and C_{20} are in units of $(\text{GeV}/c)^{-3}$, and D_0 is in units of $(\text{GeV}/c)^{-4}$. All β parameters are in units of $(\text{GeV}/c)^{-2}$. Apply powers of $\hbar c=0.197\,32$ GeV fm as necessary to obtain parameters in fm units. The tabulated amplitudes do not include the effects of the energy shift of Eq. (6).

T_{lab}	A_0	C_{10}	C_{20}	B_0	D_0	E_0
100	3.21−i5.96	−1.24−i17.50	−1.71−i16.47	−0.72+i2.65	−10.7−i388.	1.0 +i3.24
200	2.46−i3.12	−0.26−i13.18	−0.67−i12.33	0.0 +i2.02	3.0−i299.	1.55+i1.13
300	2.49−i1.99	−0.46−i10.78	−0.95−i10.00	0.0 +i1.92	1.1−i241.	1.37+i0.28
400	2.62−i1.52	−0.62−i9.28	−1.24−i8.54	−0.14+i1.81	0.4−i200.	1.10+i0.07
500	3.07−i1.27	−0.86−i8.17	−1.71−i7.44	−0.40+i1.75	−0.9−i175.	0.95−i0.48
600	3.66−i0.91	−1.29−i7.25	−2.36−i6.62	−0.42+i1.47	−3.1−i153.	0.85−i0.76
700	4.48−i0.42	−1.51−i6.53	−2.83−i6.06	−0.27+i1.30	−10.2−i134.	1.07−i0.85
800	4.81+i0.14	−1.62−i5.99	−3.07−i5.67	−0.17+i1.23	−11.5−i120.	1.01−i0.72
900	4.84+i0.57	−1.29−i5.49	−2.78−i5.29	−0.08+i1.21	−9.5−i108.	0.74−i0.63
1000	4.83+i0.61	−0.86−i4.63	−2.39−i4.52	−0.05+i0.95	−7.7−i97.8	0.54−i0.11

T_{lab}	β_A	β_{C_1}	β_{C_2}	β_B	β_D
100	13.40−i1.56	6.75−i0.88	6.32−i1.08	5.81−i2.95	40.9 −i0.93
200	13.75−i4.62	4.74−i0.36	3.99−i0.59	14.85+0.72	40.2 −i0.34
300	10.52−i7.94	4.53+i0.05	3.60−i0.17	16.47+i1.21	36.4 −i0.04
400	7.17−i7.75	4.54+i0.38	3.54−i0.17	15.61+i0.41	33.8 −i0.08
500	5.42−i5.92	4.55+i0.62	3.46+i0.30	16.60−i1.43	31.3 +i0.65
600	4.41−i4.46	4.47+i0.88	3.36+i0.37	20.16−i1.80	30.0 +i2.11
700	4.82−i3.38	4.29+i1.21	3.32+i0.29	20.47+i12.2	26.6 +i5.77
800	4.48−i2.67	4.14+i1.27	3.33+i0.23	12.54+i3.84	23.1 +i6.29
900	3.98−i2.22	4.03+i1.42	3.20+i0.39	10.23+i11.95	20.35+i5.69
1000	3.89−i1.80	4.25+i1.90	3.20+i0.73	7.39+i15.54	19.98+i5.10

TABLE V. *np* Breit frame Gaussian amplitude parameters. Units are as specified in Table IV.

T_{lab}	A_0	C_{10}	C_{20}	B_0	D_0	E_0
100	7.37−i7.45	−5.45−i14.65	−6.23−i14.16	0.84−i3.39	−10.0+i289.	1.05−i0.25
200	4.21−i2.90	−4.30−i11.31	−5.01−i11.21	−0.09−i2.33	−5.6+i133.	1.18−i1.37
300	3.64−i1.16	−3.47−i9.01	−4.24−i9.08	−0.30−i1.48	−3.0+i89.4	0.91−i1.78
400	3.39−i0.35	−2.86−i7.51	−3.70−i7.65	−0.36−i0.95	−1.9+i63.6	0.66−i1.98
500	3.52+i0.09	−2.62−i6.40	−3.58−i6.64	−0.39−i0.89	0.0+i57.7	0.49−i1.47
600	3.54+i0.54	−2.39−i5.62	−3.42−i5.90	−0.39−i0.55	−2.3+i42.4	0.42−i2.27
700	3.82+i0.96	−2.25−i4.98	−3.38−i5.38	−0.28−i0.47	−5.7+i36.2	0.50−i2.31
800	3.90+i1.37	−2.10−i4.49	−3.29−i5.00	−0.20−i0.39	−6.3+31.2	0.46−i2.18
900	3.83+i1.69	−1.78−i4.05	−2.99−i4.66	−0.14−i0.34	−5.1+i27.5	0.32−i2.03
1000	3.77+i1.79	−1.43−i3.47	−2.65−i4.16	−0.12−i0.40	−4.3+i24.2	0.22−i1.74

T_{lab}	β_A	β_{C_1}	β_{C_2}	β_B	β_D
100	11.53−i0.61	11.78−i3.87	11.59−i4.23	−2.30+i1.18	26.48−i1.23
200	14.68−i2.15	7.62−i2.02	6.96−i2.65	−8.62−i0.04	13.03−i0.46
300	11.76−i6.20	6.31−i1.02	5.43−i1.68	−11.01−i1.45	11.22−i0.11
400	7.81−i6.19	5.64−i0.38	4.67−i1.01	−11.91−i3.05	9.09+i0.23
500	6.19−i4.61	5.32−i0.40	4.45−i0.97	−8.47−i2.45	8.71+i0.16
600	4.76−i3.34	4.86+i0.34	3.97−i0.35	−9.66−i5.08	8.01+i0.26
700	4.77−i2.51	4.48+i0.66	3.78−i0.20	−9.11−i4.96	7.81+i0.04
800	4.53−i1.82	4.18+i0.77	3.67−i0.12	−8.45−i4.77	7.79−i0.16
900	4.25−i1.34	3.92+i0.89	3.50+i0.02	−7.85−i4.07	7.72−i0.14
1000	4.18−i0.97	3.82+i1.22	3.43+i0.24	−5.95−i3.10	7.67−i0.11

TABLE VI. *pp* and *np* c.m. frame Gaussian amplitude parameters. Units are as specified in Table IV.

T_{lab}	*pp* A_0	*pp* C_0	*np* A_0	*np* C_0
100	$3.21-i5.96$	$-1.47-i16.99$	$7.36-i7.45$	$-5.83-i14.41$
200	$2.46-i3.12$	$-0.46-i12.76$	$4.21-i2.90$	$-4.65-i11.27$
300	$2.49-i1.99$	$-0.70-i10.39$	$3.64-i1.16$	$-3.84-i9.06$
400	$2.62-i1.52$	$-0.92-i8.91$	$3.39-i0.35$	$-3.27-i7.59$
500	$3.07-i1.27$	$-1.27-i7.80$	$3.52+i0.09$	$-3.08-i6.53$
600	$3.66-i0.91$	$-1.79-i6.93$	$3.54+i0.54$	$-2.88-i5.76$
700	$4.48-i0.42$	$-2.13-i6.28$	$3.82+i0.96$	$-2.78-i5.18$
800	$4.81+i0.14$	$-2.29-i5.81$	$3.90+i1.37$	$-2.65-i4.74$
900	$4.84+i0.57$	$-1.96-i5.36$	$3.83+i1.69$	$-2.33-i4.34$
1000	$4.83+i0.61$	$-1.55-i4.55$	$3.77+i1.79$	$-1.98-i3.79$
T_{lab}	β_A	β_C	β_A	β_C
100	$13.40-i1.56$	$6.46-i0.97$	$11.52-i0.61$	$11.68-i4.04$
200	$13.75-i4.62$	$4.38-i0.47$	$14.68-i2.16$	$7.27-i2.32$
300	$10.51-i7.96$	$4.08-i0.04$	$11.75-i6.23$	$5.84-i1.34$
400	$7.16-i7.78$	$4.05+i0.30$	$7.78-i6.22$	$5.12-i0.68$
500	$5.40-i5.95$	$4.01+i0.50$	$6.15-i4.64$	$4.84-i0.67$
600	$4.39-i4.49$	$3.90+i0.67$	$4.72-i3.36$	$4.35+i0.0$
700	$4.79-i3.40$	$3.76+i0.79$	$4.72-i2.53$	$4.06+i0.22$
800	$4.45-i2.70$	$3.67+i0.78$	$4.48-i1.85$	$3.85+i0.30$
900	$3.94-i2.24$	$3.55+i0.94$	$4.19-i1.36$	$3.64+i0.42$
1000	$3.85-i1.82$	$3.62+i1.35$	$4.13-i0.99$	$3.55+i0.68$

dependence is not Gaussian and thus the corresponding β_E parameters have been omitted from Tables IV and V.

For comparison, some of the c.m. frame amplitudes of Eq. (7) are given in Table VI. Owing to the convention of dividing out the momentum from both f_B and f_c, the forward amplitudes A_0, B_0, and E_0 are invariants (see also the discussion in Ref. 2). Furthermore, the rotation angles X and ρ defined by Eqs. (19) and (20) tend to zero as $q \rightarrow 0$. Thus the Wigner rotation only effects the spin flip amplitudes C_1 and C_2 and the Gaussian falloff parameters β as may be seen by comparison of the tables. The effects are largest when q^2 is largest. Sizable differences have been observed in calculations of proton elastic scattering by light ions due to the energy shift of Eq. (6), however, the Wigner rotation of Eq. (16) seems to yield $\simeq 6\%$ effects in spin observables for $\vec{p}+\vec{d}$ elastic scattering. Very large differences between c.m. and Breit frame *NN* amplitudes have been demonstrated in Ref. 5 for cases where q in proton-nucleus scattering corresponds to *NN* scattering angles exceeding 90° at the beam kinetic energy. This occurs for $\theta > 60°$ in p-^{4}He scattering.

For proton scattering by heavy nuclei, the form factor $S(q)$ suppresses the large q values and thus only minor differences are observed due to the difference between c.m. and Breit frame *NN* amplitudes. This conclusion is documented by calculations based on the Kerman-McManus-Thaler (KMT) optical potential formalism as shown in Figs. 3 and 4. Figure 3 shows the analyzing power for 500 MeV p-^{40}Ca elastic scattering as a function

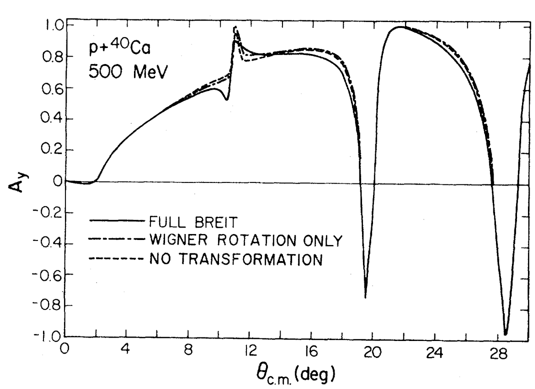

FIG. 3. Impulse approximation calculations for 500 MeV $p+^{40}$Ca. Analyzing power using *NN* amplitudes: (1) in the Breit frame, Eq. (16) (solid curve); (2) using the Wigner rotation only (no energy shift, dashed-dotted curve); and (3) with neither of these effects (dashed curve).

TABLE VII. Results for root mean square neutron radii deduced from elastic proton scattering as in Ref. 13.

		$\langle r_n^2 \rangle^{1/2}$(fm)
	Full Breit	3.048
^{40}Ca, 500 MeV	Wigner rotation	2.971
	No transformation	2.995
^{12}C, 800 MeV	Full Breit	2.127
	No transformation	2.081
	Full Breit	3.234
^{40}Ca, 800 MeV	Wigner rotation	3.201
	No transformation	3.214

of the center-of-mass scattering angle. The calculations labeled "full Breit" were made on the basis of Eqs. (6) and (16) using an interpolation of the energy dependence of the *NN* phase shifts in order to account for the energy increase with q^2. The results labeled "Wigner rotation only" are based on ignoring the energy increase and thus include only the rotation as in Eq. (30). Neither of these effects is very large, as can be seen by comparison with the dashed

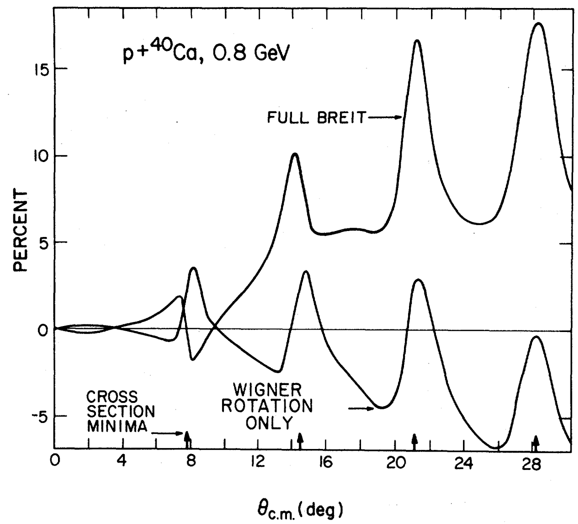

FIG. 4. Percentage differences for 800 MeV $p+{}^{40}$Ca differential cross sections using the impulse approximation *NN* amplitudes in the Breit frame, and with the Wigner spin rotation only, compared to calculations with *NN* amplitudes omitting these effects.

TABLE VIII. *pp* and *np* invariant amplitude Gaussian parameters. Forward amplitudes $\mathcal{F}_{S0}$ and $\mathcal{F}_{V0}$ are Gaussian falloff parameters and are in units of $(\text{GeV}/c)^{-2}$. Owing to the convention of Eq. (7), a factor $2ik_c$ must be applied to convert these amplitudes to c.m. frame scattering amplitudes.

	pp		*np*	
T_{lab}	$\mathcal{F}_{S0}$	$\mathcal{F}_{V0}$	$\mathcal{F}_{S0}$	$\mathcal{F}_{V0}$
100	$-9.18-i94.10$	$11.20+i79.66$	$-25.12-i68.30$	$29.35+i54.99$
200	$-3.73-i46.91$	$5.11+i36.10$	$-15.43-i36.56$	$16.19+i27.74$
300	$-2.68-i31.26$	$3.92+i22.18$	$-10.19-i24.10$	$10.48+i17.38$
400	$-2.16-i24.09$	$3.35+i15.82$	$-7.26-i17.75$	$7.47+i12.20$
500	$-2.25-i19.13$	$3.47+i11.65$	$-5.89-i14.68$	$6.14+i9.64$
600	$-2.74-i15.85$	$3.91+i9.12$	$-4.96-i11.23$	$5.18+i7.18$
700	$-2.91-i13.55$	$4.23+i7.53$	$-4.35-i9.39$	$4.68+i5.93$
800	$-2.80-i11.96$	$4.11+i6.53$	$-3.80-i8.13$	$4.15+i5.13$
900	$-1.74-i10.55$	$3.36+i5.68$	$-2.90-i7.09$	$3.44+i4.48$
1000	$-0.64-i9.02$	$2.65+i4.66$	$-2.05-i6.03$	$2.82+i3.78$
T_{lab}	β_S	β_V	β_S	β_V
100	$4.55-i1.07$	$3.25-i1.44$	$1.41-i7.03$	$0.99-i8.74$
200	$3.23-i0.41$	$1.69-i0.85$	$0.16-i4.26$	$-0.52-i5.90$
300	$3.33+i0.06$	$1.70-i0.34$	$0.49-i2.77$	$-0.23+i4.16$
400	$3.94+i0.41$	$2.26+i0.11$	$0.80-i1.85$	$0.12-i3.03$
500	$3.72+i0.47$	$2.06+i0.06$	$1.90-i1.36$	$1.31-i2.34$
600	$3.78+i0.47$	$2.20-i0.05$	$1.20-i1.17$	$0.88-i2.07$
700	$3.85+i0.29$	$2.55-i0.51$	$1.36-i1.08$	$1.32-i1.94$
800	$3.93+i0.20$	$2.80-i0.57$	$1.54-i0.95$	$1.66-i1.66$
900	$3.89+i0.46$	$2.70-i0.28$	$1.52-i0.60$	$1.71-i1.28$
1000	$3.93+i0.85$	$2.63+i0.05$	$1.39-i0.20$	$1.72-i0.97$

curve which includes neither the energy shift nor the Wigner rotation, but obviously the energy shift is more important.

Figure 4 shows similar results for the 800 MeV p-^{40}Ca elastic scattering cross section where the small differences are shown as percentage changes of the cross section. Again the effects are not large. Table VII summarizes the effects of the use of Breit frame amplitudes on the neutron root-mean-square (rms) radii determined by fitting proton-nucleus elastic scattering as in Ref. 13.

Table VIII lists Gaussian amplitude parameters for the scalar and vector invariant amplitudes of Eq. (8), for example,

$$\mathscr{F}_S(q)=\mathscr{F}_{S0}\exp(-\beta_S q^2)$$

and

$$\mathscr{F}_V(q)=\mathscr{F}_{V0}\exp(-\beta_V q^2)\ .$$

The scalar and vector amplitudes $\mathscr{F}_{S0}$ and $\mathscr{F}_{V0}$ have opposite signs and are considerably larger in magnitude than the corresponding forward amplitudes in the Pauli representation. These differences can be traced back to the influence of the Pauli C amplitude of Eq. (7) through the transformation of Eq. (12). The amplitudes $\mathscr{F}_{S0}$ and $\mathscr{F}_{V0}$ determine the impulse approximation Dirac optical potential as is explained in Ref. 11.

For proton scattering by nuclei, the Breit frame amplitudes are the natural ingredients of calculations based on the impulse approximation. These amplitudes differ from the c.m. amplitudes because of the energy shift Eq. (6) and the Wigner rotation of spins. For heavy nuclei these differences produce only slight changes to the observed scattering, however, results for light ions show much larger effects at high q^2. One of the reasons for the larger effect in light ion scattering is that the single scattering term remains influential at large q^2 and the energy shift in Eq. (6) can become quite large.

As a by-product of the derivation of a transformation between c.m. and Breit frames, we have derived a general matrix relation, Eq. (12), from which the invariant Dirac amplitudes of Eq. (8) can be calculated directly from the NN phase shifts.

The support of the U. S. Department of Energy for this research is gratefully acknowledged.

[1]L. Ray *et al.*, Phys. Rev. C 23, 828 (1981).

[2]Recent references to proton-nucleus analyses are given in S. J. Wallace, in *Advances in Nuclear Physics,* edited by J. Negele and E. Vogt (Plenum, New York, 1981), Vol. 12, p. 135.

[3]S. A. Gurvitz, J.-P. Dedonder, and R. D. Amado, Phys. Rev. C 19, 142 (1979).

[4]S. A. Gurvitz, Phys. Rev. C 20, 1256 (1979).

[5]S. A. Gurvitz, Y. Alexander, and A. S. Rinat, Ann. Phys. (N.Y.) 93, 152 (1975); 98, 346 (1976).

[6]J. A. McNeil, Ph.D. dissertation, University of Maryland, 1979 (unpublished).

[7]G. Alberi, M. Bleszynski, T. Jaroszewicz, and S. Santos, Ann. Phys. (N.Y.) 142, 299 (1982).

[8]N. Hoshizaki, Prog. Theor. Phys. Suppl. (Jpn.) 42, 107 (1968); J. Bystricky, F. Lehar, and P. Winternitz, J. Phys. (Paris) 39, 1 (1978).

[9]M. L. Goldberger, Y. Nambu, and R. Oehme, Ann. Phys. (N.Y.) 2, 226 (1957).

[10]J. Bjorken and S. Drell, *Relativistic Quantum Mechanics* (McGraw-Hill, New York, 1964), Vol. I, p. 30.

[11]J. A. McNeil, J. R. Shepard, and S. J. Wallace (unpublished).

[12]R. Arndt, L. D. Roper, R. A. Bryan, R. B. Clark, B. J. VerWest, and P. Signell, Virginia Polytechnic Institute and State University Report VPISA-2(82), 1982.

[13]L. Ray, Phys. Rev. C 19, 1855 (1979).